

Stein EWMA Control Charts for Count Processes

Christian H. Weiß^{*†}

January 23, 2024

Abstract

The monitoring of serially independent or autocorrelated count processes is considered, having a Poisson or (negative) binomial marginal distribution under in-control conditions. Utilizing the corresponding Stein identities, exponentially weighted moving-average (EWMA) control charts are constructed, which can be flexibly adapted to uncover zero inflation, over- or underdispersion. The proposed Stein EWMA charts' performance is investigated by simulations, and their usefulness is demonstrated by a real-world data example from health surveillance.

KEY WORDS: attributes data; average run lengths; count time series; EWMA control charts; Stein identity

1 Introduction

The sequential monitoring of count processes $(X_t)_{t \in \mathbb{N} = \{1, 2, \dots\}}$ (i. e., where the X_t have a quantitative range contained in $\mathbb{N}_0 = \{0, 1, \dots\}$) is of utmost importance in many application areas, such as the quality control of manufactured items (counts of defects or non-conformities) or health surveillance (counts of infections or hospital admissions); see Montgomery (2009); Weiß (2015, 2018) for examples and references. The primary tool for managing statistical process control (SPC) for (X_t) is the use of attributes control charts. These charts involve plotting specific statistics sequentially until signals indicate the necessity for corrective action. These statistics are computed in an online manner from the sequence of incoming counts (X_t) . The control

^{*}Helmut Schmidt University, Department of Mathematics and Statistics, Hamburg, Germany.

[†]Corresponding author. E-Mail: weissc@hsu-hh.de. ORCID: 0000-0001-8739-6631

chart triggers a signal (“alarm”) if the plotted statistic violates the specified control limits (CLs). The CLs are derived from the so-called in-control model of (X_t) , i. e., a stochastic model that assumes (X_t) to operate under stable conditions. Hence, an alarm (a violation of the CLs) is interpreted as an indication of a possible process deterioration (out-of-control situation). Therefore, if the alarm occurs when the process (X_t) is genuinely out of control, it is considered a true alarm. On the other hand, an alarm under in-control conditions is regarded as a false alarm. It stands to reason that CLs should be chosen to avoid false alarms for as long as possible, and to receive a true alarm as soon as possible. The default metric for evaluating these durations until alarm is the average run length (ARL), i. e., the expected number of plotted statistics until the first alarm. For a more detailed description of the aforementioned terms and concepts as well as for further references, the reader may consult SPC textbooks such as Montgomery (2009); Qiu (2014). Various control charts for diverse count processes have been developed during the last decades, covering serially independent or autocorrelated counts, and counts having full \mathbb{N}_0 as their range (unbounded counts) or just the finite subset $\{0, \dots, n\}$ with specified $n \in \mathbb{N}$ (bounded counts). The most simple type of control chart is obtained by plotting the counts X_t themselves against appropriately chosen CLs, which is called a *c*-chart if monitoring unbounded counts and an *np*-chart for bounded counts. Such types of Shewhart control chart can be classified as being memory-less as the t th plotted statistic does not comprise information about earlier counts (at least not beyond the mere effect of autocorrelation). Consequently, while Shewhart charts might be quick in detecting a sudden strong process shift, they are slow in detecting small process changes. Therefore, also several memory-type control charts for counts have been proposed, where in the present research, our focus is on exponentially weighted moving-average (EWMA) charts. Some recent references on EWMA-type control charts for counts are Gan (1990); Borrór et al. (1998); Weiß (2011); Rakitzis et al. (2015); Morais et al. (2018); Morais & Knoth (2020); Anastasopoulou & Rakitzis (2022a,b). Further references (also on other types of count control charts) can be found in Weiß (2015, 2018); Alevizakos & Koukouvinos (2020). The default version of the EWMA chart plots the statistics

$$Z_0 = \mu_0, \quad Z_t = \lambda \cdot X_t + (1 - \lambda) \cdot Z_{t-1} \quad \text{for } t = 1, 2, \dots \quad (1)$$

against a specified lower and upper CL (LCL and UCL, respectively), where $\mu_0 > 0$ denotes the in-control mean of (X_t) . The smoothing parameter $\lambda \in (0, 1]$ in (1) controls the strength of the memory (the smaller λ , the stronger the memory). If $\lambda = 1$, then (1) reduces to the *c*- or *np*-chart, respectively.

All the aforementioned count EWMA charts are mainly designed to detect shifts in the process mean, although they may sometimes (“accidentally”) also react to increases in variance or changes in the autocorrelation structure. In the present research, however, our focus is on “more sophisticated” out-of-control scenarios, namely where the mean changes together with further distributional properties (i. e., where the process change cannot be traced back to a sole change in the mean parameter), or where “purely distributional changes” (not affecting the mean) happen. Such “distributional changes” might be increases or decreases in dispersion compared to the in-control model (overdispersion or underdispersion, respectively), or an excessive number of zero counts (zero inflation), to mention those being most relevant in practice. The basic idea of our approach is as follows. Many common count distributions can be characterized by a type of moment identity, referred to as *Stein identity*, which has to hold for a large class of functions (e. g., all bounded functions on \mathbb{N}_0). The idea to develop such identities dates back to Stein (1972, 1986), and further contributions and references can be found in Sudheesh (2009); Sudheesh & Tibiletti (2012); Landsman & Valdez (2016). Recently, such Stein identities were successfully used to develop powerful goodness-of-fit (GoF) tests for counts, see Betsch et al. (2022); Weiß et al. (2023) for Stein-type GoF-tests for independent and identically distributed (i. i. d.) counts, and Aleksandrov et al. (2022a,b) for tests for count time series. Thus, it suggests itself to utilize these Stein identities also for developing sequential test procedures, namely count control charts for relevant types of in-control model. In a first research (see Weiß, 2023), this idea was tried for the special case of i. i. d. Poisson counts, and the achieved ARL performance was quite appealing. This motivates to develop and investigate Stein-based control charts for count data on a much broader scale, namely for various different count distributions and not only for i. i. d. but also for time series data. More precisely, we focus on the three most common count distributions in practice, namely Poisson (Poi), negative binomial (NB), and binomial (Bin), and we include first-order autoregressive (AR(1)) models having either Poi-, NB-, or Bin-distributed marginal distributions in our research.

The outline of this chapter is as follows. In Section 2, we briefly present the count models used for this research, and we provide the Stein identities for the Poi-, NB-, and Bin-distribution. These are used in Section 3 to construct novel EWMA-type control charts for counts, where the chart design with respect to diverse out-of-control scenarios is discussed in detail. In Section 4, results from a simulation study are presented, which allow to analyze the Stein EWMA charts’ ARL performance. Section 5 then investigates a real-world data example on registrations in the emergency department of a

children’s hospital, which illustrates the application and interpretation of the novel Stein EWMA charts in practice. Finally, Section 6 concludes the article and discusses possible directions for future research.

2 Count Models and Stein Identities

The two most common distributions for unbounded counts are the Poi- and NB-distribution, while the Bin-distribution is the default choice for bounded counts; see Johnson et al. (2005) for details and properties. The $\text{Poi}(\mu)$ -distribution with mean $\mu > 0$ is known to be equidispersed, i. e., its variance σ^2 satisfies $\sigma^2 = \mu$. By contrast, $\text{NB}(\nu, \frac{\nu}{\nu+\mu})$ with $\nu, \mu > 0$ exhibits overdispersion relative to the Poi-distribution, because its variance $\sigma^2 = (1 + \frac{\mu}{\nu})\mu$ always exceeds the mean. The $\text{Bin}(n, \mu/n)$ -distribution with $n \in \mathbb{N}$ and $\mu \in (0, n)$, in turn, refers to counts having the bounded range $\{0, \dots, n\}$.

There is a huge variety of time series models related to the Poi-, NB-, or Bin-distribution, see Weiß (2018) for a comprehensive overview. Here, many models use a *conditional* Poi-, NB-, or Bin-distribution (regression models) while the marginal distribution does not belong to any parametric model family. However, to be able to apply a Stein identity to given data, we need to specify the corresponding *marginal* distribution. Regarding the count time series models proposed so far Weiß (2018), only a considerably smaller number of models has a Poi-, NB-, or Bin-*marginal* distribution. For the sake of studying possible effects of serial dependence on the charts’ performance, we shall consider three of the AR(1)-type processes surveyed by Weiß (2008), whose model definitions use so-called thinning operators as integer substitutes of the multiplication:

- the Poi-INAR(1) process (integer AR) defined by

$$X_t = \rho \circ X_{t-1} + \epsilon_t \quad \text{with i. i. d. } \epsilon_t \sim \text{Poi}(\mu(1 - \rho)), \quad (2)$$

- the NB-IINAR(1) process (iterated-thinning INAR) defined by

$$X_t = \rho \otimes_{\pi} X_{t-1} + \epsilon_t \quad \text{with i. i. d. } \epsilon_t \sim \text{NB}(\nu, \pi) \text{ and } \pi = \frac{\nu}{\mu(1-\rho)+\nu}, \quad (3)$$

- the BinAR(1) process defined by

$$X_t = \alpha \circ X_{t-1} + \beta \circ (n - X_{t-1}) \quad \text{with } \beta = (1 - \rho) \frac{\mu}{n}, \alpha = \beta + \rho. \quad (4)$$

Definitions (2) and (4) use the binomial thinning operator, which is defined by requiring a conditional Bin-distribution, namely $\theta \circ X|X \sim \text{Bin}(X, \theta)$ for $\theta \in (0, 1)$. Definition (3), in turn, uses iterated thinning defined as $\rho \circledast_{\pi} X = \sum_{i=1}^{(\pi\rho) \circ X} Y_i$, where the counting series (Y_i) is i. i. d. according to $Y_i \sim 1 + \text{NB}(1, \pi)$. The crucial point for the subsequent research is the following:

Models (2)–(4) lead to stationary Markov chains with AR(1)-like autocorrelation function (ACF) $\rho(h) = \rho^h$ for time lags $h \in \mathbb{N}$, where $\rho \in (0, 1)$ for all three models. The stationary marginal distributions are $\text{Poi}(\mu)$, $\text{NB}(\nu, \frac{\nu}{\nu+\mu})$, and $\text{Bin}(n, \mu/n)$, respectively, see Weiß (2008). The parameter ρ allows to control the extent of serial dependence, where the boundary case $\rho \rightarrow 0$ leads to i. i. d. counts.

Independent of the value of ρ , we are always concerned with a Poi-, NB-, or Bin-marginal distribution. Any of these three distributions is uniquely characterized by a corresponding Stein identity, see Sudheesh & Tibiletti (2012):

- $X \sim \text{Poi}(\mu)$ if and only if

$$E[X f(X)] = \mu E[f(X + 1)] \quad (5)$$

holds for all bounded functions $f : \mathbb{N}_0 \rightarrow \mathbb{R}$;

- $X \sim \text{NB}(\nu, \frac{\nu}{\nu+\mu})$ if and only if

$$(\nu + \mu) E[X f(X)] = \mu E[(\nu + X) f(X + 1)] \quad (6)$$

holds for all bounded functions $f : \mathbb{N}_0 \rightarrow \mathbb{R}$;

- $X \sim \text{Bin}(n, \mu/n)$ if and only if

$$(n - \mu) E[X f(X)] = \mu E[(n - X) f(X + 1)] \quad (7)$$

holds for all bounded functions $f : \mathbb{N}_0 \rightarrow \mathbb{R}$.

Identity (5) is commonly referred to as the Stein–Chen identity (see Chen, 1975). Note that the identities (5)–(7) constitute non-trivial statements only if f is not constant on \mathbb{N}_0 , and if f is not identical to zero on \mathbb{N} .

In the subsequent Section 3, we shall derive control charts from the identities (5)–(7). As these identities have to hold for all bounded functions f under in-control conditions, we can select any choice of f for defining the control charts. This degree of freedom can be used to achieve particular sensitivity regarding a specified type of out-of-control scenario.

3 Stein EWMA Charts for Counts

The three identities (5)–(7) always depend on three types of moment: the mean μ , the moment $E[X f(X)]$, and a moment involving $f(X + 1)$. The idea of the GoF-tests in Aleksandrov et al. (2022a,b); Weiß et al. (2023) as well as of the Poisson EWMA charts in Weiß (2023) was to derive a statistic by solving the identities in a certain way, and to substitute the involved population moments by appropriate types of sample moments. In Weiß (2023), two types of constructing an EWMA control chart were analyzed, and it turned out that one of these types is clearly superior, namely the one called “ABC-EWMA chart”. Building on this experience, we propose the following Stein EWMA charts for sequentially monitoring Poi-, NB-, or Bin-counts, respectively, where $E_0[\cdot]$ expresses that the expectation is computed with respect to the in-control model. For all three Stein EWMA charts, we compute

$$\begin{aligned} A_0 &= E_0[X f(X)], & A_t &= \lambda \cdot X_t f(X_t) + (1 - \lambda) \cdot A_{t-1}, \\ C_0 &= \mu_0, & C_t &= \lambda \cdot X_t + (1 - \lambda) \cdot C_{t-1}, \quad \text{for } t = 1, 2, \dots \end{aligned} \quad (8)$$

Furthermore, we compute for the

- Poi(μ_0) in-control model:

$$\begin{aligned} B_0 &= E_0[f(X + 1)], & B_t &= \lambda \cdot f(X_t + 1) + (1 - \lambda) \cdot B_{t-1}, \\ Z_0^S &= 1, & Z_t^S &= \frac{A_t}{B_t C_t}, \quad \text{for } t = 1, 2, \dots; \end{aligned} \quad (9)$$

- NB($\nu, \frac{\nu}{\nu + \mu_0}$) in-control model:

$$\begin{aligned} B_0 &= E_0[(\nu + X) f(X + 1)], \\ B_t &= \lambda \cdot (\nu + X_t) f(X_t + 1) + (1 - \lambda) \cdot B_{t-1}, \\ Z_0^S &= 1, & Z_t^S &= \frac{(\nu + C_t) A_t}{B_t C_t}, \quad \text{for } t = 1, 2, \dots; \end{aligned} \quad (10)$$

- Bin($n, \mu_0/n$) in-control model:

$$\begin{aligned} B_0 &= E_0[(n - X) f(X + 1)], \\ B_t &= \lambda \cdot (n - X_t) f(X_t + 1) + (1 - \lambda) \cdot B_{t-1}, \\ Z_0^S &= 1, & Z_t^S &= \frac{(n - C_t) A_t}{B_t C_t}, \quad \text{for } t = 1, 2, \dots \end{aligned} \quad (11)$$

We define the respective *Stein EWMA chart* by plotting the statistics Z_t^S against appropriately chosen $LCL < 1 < UCL$, where we expect Z_t^S to vary closely around 1 under in-control assumptions.

The actual chart design now comprises two steps. First, we have to select the function f involved in (8)–(11). Here, one could generally choose any bounded function on \mathbb{N}_0 , recall (5)–(7), except trivial choices like f being constant on \mathbb{N}_0 , or $f \equiv 0$ on \mathbb{N} . But not any choice of f will lead to an appealing chart performance. Instead, f has to be chosen with respect to the anticipated out-of-control scenario, in an analogous way as proposed by Alexandrov et al. (2022a,b); Weiß et al. (2023) and Weiß (2023). The idea is to interpret f as a weight function within the “A- and B-moments”, which puts unequal weight on the integers in \mathbb{N}_0 . For a given anticipated out-of-control scenario, one should put most weight on those regions of \mathbb{N}_0 where one gets the strongest departures from the in-control model. If we want to uncover zero inflation, for example, we should choose an f with relatively large weight close to zero counts, whereas for “general” overdispersion (i. e., if the probability mass function (PMF) is flattened compared to the in-control model), it is advantageous to put more weight on large counts. So in accordance to the recommendations in Weiß (2023), the following choices of f are considered in these two cases:

- for uncovering overdispersion relative to the in-control model, we use the linear weights $f(x) = |x - 1|$;
- for uncovering zero inflation relative to the in-control model, we use the root weights $f(x) = |x - 1|^{1/4}$.

The case of underdispersion has not been investigated by Weiß (2023). Thus, as a starting point, we follow the findings of Weiß et al. (2023) on GoF-tests and

- for uncovering underdispersion relative to the in-control model, we use the inverse weights $f(x) = 1/(x + 1)$.

The described approach for choosing the weight function is later illustrated in some more detail when discussing Figure 1. The ARL performance of the aforementioned choices of f is analyzed in Section 4 below. As we shall see, the underdispersion scenario is much more demanding than overdispersion or zero inflation. Therefore, further choices for f shall be considered later in Section 4.2.

After having specified f , the second step of chart design is the choice of the triple (λ, LCL, UCL) . Assume for the moment that the smoothing parameter λ has already been fixed. Then, LCL and UCL are determined based

on ARL considerations. While different ARL concepts exist in the literature (Knoth, 2006), it is common to use the zero-state ARL for evaluating the in-control performance. The most simple solution (the one used here) are symmetric CLs of the form $LCL = 1 - L$ and $UCL = 1 + L$, where L is chosen such that the desired in-control ARL (ARL_0) is met in close approximation (the textbook choice is the target value 370). Alternatively, one could define asymmetric CLs by also considering the out-of-control ARL performance, but this is only reasonable if a particular out-of-control scenario has been fixed. For example, if one assumes that the out-of-control models differ from the in-control one solely in terms of the mean μ , then asymmetric CLs may allow to obtain an unbiased ARL performance with respect to μ , i. e., the ARL as a function of μ is maximal in the in-control mean μ_0 and decreases symmetrically around μ_0 , see Section 4 in Morais & Knoth (2020). But as we shall consider a broad variety of out-of-control scenarios, we restrict to symmetric CLs here, i. e., $\mu_0 \mp L$ for ordinary EWMA and $1 \mp L$ for Stein EWMA charts.

At this point, let us recall that the above approach for choosing f assumes that we have specified a *single* relevant out-of-control scenario, such as “zero inflation”. If the application context allows for *various* out-of-control scenarios (e. g., if underdispersion could also be possible), one can run multiple Stein EWMA charts in parallel, each designed for a different type of deterioration. This is later done in Section 5 when monitoring the emergency counts. There, one Stein EWMA chart is designed to detect overdispersion, another one for zero inflation, and a third one for underdispersion. Then, the observed pattern of alarms enables a kind of targeted diagnosis. For example, if the “zero inflation”-chart is the first to trigger an alarm, we conclude that we might be confronted with zero inflation (rather than with underdispersion etc.). Certainly, if running many charts in parallel, the risk increases that one of these charts gives a false alarm (“multiple testing”). Generally, the risk of false alarms is controlled by setting a target value ARL_0 for the in-control ARL. As described before, in our simulation study, we set $ARL_0 \approx 370$ for each single chart for comparability. But if multiple control charts are applied simultaneously, it would also be possible to determine their CLs such that the *joint* in-control ARL meets a target value, i. e., the ARL would be defined as the expected time until one of the charts triggers the first alarm.

Another remark refers to the choice of the smoothing parameter λ . To ensure a sufficient memory, one often chooses small values for λ , such as $\lambda \in \{0.25, 0.10, 0.05\}$. The actual choice of λ might be done based on out-of-control ARLs. For example, we could first compute several candidate triples $(\lambda_i, LCL_i, UCL_i)$ having the same ARL_0 . Then, we fix a specified out-of-

control scenario and select that triple where the corresponding out-of-control ARL is closest to a given target value. In this way, one might end up with different λ for different Stein EWMA charts. But as we choose $f(x)$ with respect to different out-of-control scenarios, comparable chart designs are most easily obtained by a unique λ . Furthermore, all Stein EWMA charts follow the same type of recursive scheme, which makes it plausible to use a unique value for λ . Thus, in the sequel, we follow the practice in Weiß (2023) and set $\lambda = 0.10$ throughout our analyses.

Let us conclude this section with a note on out-of-control ARLs. As mentioned before, there are a couple of competing ARL concepts for evaluating a control chart's out-of-control performance, see Knoth (2006), which are typically defined with respect to different positions of the change point. Here, the change point τ expresses the time where the process turns out of control, i. e., the process is in control (out of control) for $t < \tau$ ($t \geq \tau$). The out-of-control zero-state ARL assumes that the process change happens right at the beginning of process monitoring, i. e., the change point equals $\tau = 1$. The conditional expected delay $\text{CED}(\tau)$, by contrast, assumes a later change point $\tau > 1$, where the limit $\tau \rightarrow \infty$ leads to the steady-state ARL. While $\tau = 1$ would happen for a misspecified in-control model, late change points are often more realistic in practice (but one does not know the true value of τ in advance). Fortunately, it turned out in the initial analyses of Weiß (2023) that the exact position of τ does not have a substantial effect on the computed out-of-control ARL values, i. e., the Stein EWMA charts showed roughly the same performance for early and late process changes. Since the charts of the present study are defined in complete analogy to those of Weiß (2023), we expect the value of the zero-state ARL to be representative also for $\tau > 1$ (for “problematic” types of control chart, see the discussion in Knoth et al. (2023)). For this reason, we restrict our subsequent analyses to zero-state ARLs, and these are computed based on simulations. So one simulates the considered process for R times (we use $R = 10^4$), applies the specified control chart to it, and determines the time until the first alarm. In this way, one gets R run lengths l_1, \dots, l_R , and the sample mean thereof provides an approximate value of the actual ARL.

4 Simulation-based Performance Analyses

4.1 Overdispersion or Zero Inflation

Let us start our performance analyses with the case of overdispersion or zero inflation (compared to the in-control model). Strictly speaking, a zero-

inflated distribution also exhibits increased dispersion, but this increase is caused by a single point mass in zero. With overdispersion, by contrast, we refer to a flattened PMF compared to the in-control model's PMF. For unbounded counts, we use the NB-distribution for generating overdispersion, and the zero-inflated Poisson (ZIP) distribution for zero inflation. In the bounded-counts case, we use the beta-binomial (BB) distribution for overdispersion and the zero-inflated binomial (ZIB) distribution for zero inflation, see Appendix A in Weiß (2018) for details on these distributions. For the sake of a unique representation, we specify any of the aforementioned models by the mean μ and by an appropriate dispersion index, namely by $I_P = \sigma^2/\mu$ for unbounded counts and $I_B = n\sigma^2/(\mu(n - \mu))$ for bounded counts. Note that $I_P = 1$ for the Poi-distribution while $I_P > 1$ for NB and ZIP. Analogously, $I_B = 1$ for the Bin-distribution and $I_B > 1$ for BB and ZIB. The in-control means are set at either $\mu_0 = 2$ (low counts) or $\mu_0 = 5$ (medium counts). The data-generating process (DGP) produces either i. i. d. counts ($\rho = 0$) or AR(1)-like counts with $\rho = 0.5$, recall (2)–(4). The simulated ARLs rely on 10^4 replications, the target value for ARL_0 is 370.

As the case of overdispersion or zero inflation relative to an in-control Poi-distribution was already analyzed by Weiß (2023), we restrict our subsequent analyses to in-control NB- and Bin-models, see Tables 1–2 for the obtained results. The Bin-results are quite close to the Poi-results anyway, which is not surprising as these distributions are related to each other by the Poisson limit theorem. Let us start our discussion with the Bin-case in Table 1. The design of this table (and of any further table) is as follows. It consists of twelve 3×3 -blocks with a negative (positive) mean shift on the left (right) and no mean shift in the center column. In the Bin-rows, the binomial distribution is preserved, whereas we have distributional changes in the ZIB- and BB-rows. Note that at the bottom of each table, there is a scheme for interpreting the ARLs within each block. Part (a) of each table refers to i. i. d. counts, part (b) to AR(1)-like counts. Note that the BB- and ZIB-AR(1) model are constructed as in (3.27) of Weiß (2018) by replacing the Bin-thinnings in (4) by BB- or ZIB-thinnings, respectively. Finally, the first column of blocks always refers to the ordinary EWMA chart (1), whereas the remaining two columns refer to Stein EWMA charts, i. e., to (11) in case of Table 1.

Part (a) of Table 1 just confirms the findings of Weiß (2023) for the Poi-case. If we are concerned with the textbook situation, i. e., if there is a change solely in the mean parameter (the distribution is preserved otherwise), then the ordinary EWMA chart is clearly the best choice. But if there is an additional distributional change, or even only a distributional change while the mean is

Table 1: Simulated ARLs of ordinary EWMA and Stein EWMA chart for Bin-counts with $n = 10$. BB and ZIB with $I_B = 5/3$.

μ_0	$\mu =$	$\mu_0 - 0.25$	μ_0	$\mu_0 + 0.25$	$\mu_0 - 0.25$	μ_0	$\mu_0 + 0.25$	$\mu_0 - 0.25$	μ_0	$\mu_0 + 0.25$		
(a) i. i. d. counts												
		EWMA			<i>0.7805</i>	EWMA ^S $ x - 1 $			<i>0.534</i>	EWMA ^S $ x - 1 ^{1/4}$		<i>0.4235</i>
2	ZIB	69.2	87.9	51.6	22.7	26.1	29.2	16.6	19.1	21.9		
	Bin	171.5	370.2	99.3	240.2	369.5	550.6	191.5	370.6	671.0		
	BB	71.5	90.0	51.8	25.9	29.2	33.3	30.8	40.5	55.6		
		EWMA			<i>0.974</i>	EWMA ^S $ x - 1 $			<i>0.2115</i>	EWMA ^S $ x - 1 ^{1/4}$		<i>0.0511</i>
5	ZIB	69.2	87.9	51.6	18.9	19.9	20.6	12.9	14.0	15.5		
	Bin	162.5	369.5	164.1	307.2	370.1	443.4	311.5	369.5	417.2		
	BB	66.7	88.2	66.3	25.1	26.9	29.0	27.4	28.9	30.3		
(b) AR(1) counts with $\rho = 0.5$												
		EWMA			<i>1.191</i>	EWMA ^S $ x - 1 $			<i>0.639</i>	EWMA ^S $ x - 1 ^{1/4}$		<i>0.568</i>
2	ZIB	77.9	73.8	55.8	22.9	24.3	25.3	23.8	26.9	30.0		
	Bin	384.8	370.1	158.0	247.1	369.7	554.4	211.9	371.2	634.3		
	BB	105.0	105.7	77.2	33.0	39.5	47.0	44.7	58.9	77.1		
		EWMA			<i>1.493</i>	EWMA ^S $ x - 1 $			<i>0.225</i>	EWMA ^S $ x - 1 ^{1/4}$		<i>0.0528</i>
5	ZIB	30.8	29.9	28.0	7.9	7.7	7.3	7.1	6.9	6.5		
	Bin	258.0	369.1	257.3	316.7	370.9	424.1	293.9	370.9	421.8		
	BB	86.3	96.1	85.9	35.3	37.6	39.5	37.9	39.4	40.7		

Notes: In-control ARL printed in bold font, CL L shown in italic font.
 “EWMA” = ordinary EWMA; “EWMA^S” = Stein EWMA,
 where weight functions $f(x) = |x - 1|$ and $|x - 1|^{1/4}$.

Interpretation:	sole mean change	pure distrib. change	zero inflation
			overdispersion

kept fixed, then the Stein EWMA charts become superior. More precisely, if we are concerned with overdispersion (BB-model), then the weight function $f(x) = |x - 1|$ leads to the lowest ARLs, whereas zero inflation is best detected using $f(x) = |x - 1|^{1/4}$. It should be noted that we draw the same conclusions from part (a) of Table 2, which refers to the NB-case (in-control level of dispersion is $I_P = 5/3$) with Stein EWMA chart (10). There, overdispersion (relative to the in-control model) was generated by an NB-distribution with higher dispersion, namely $I_P = 5/2$, whereas we used the ZIP-distribution with $I_P = 5/3$ for causing zero inflation. Thus, we generally conclude that if monitoring i. i. d. counts and if being concerned with overdispersion under out-of-control conditions, the Stein EWMA chart with $f(x) = |x - 1|$ is the best choice, whereas $f(x) = |x - 1|^{1/4}$ performs best under zero inflation. If the type of out-of-control situation is not clear in advance, it is recommended to run all three charts of Tables 1–2 simultaneously. As these charts show a

Table 2: Simulated ARLs of ordinary EWMA and Stein EWMA chart for NB-counts with $I_P = 5/3$. ZIP with $I_P = 5/3$, and overdispersed NB (“oNB”) with $I_P = 5/2$.

μ_0	$\mu =$	$\mu_0 - 0.25$	μ_0	$\mu_0 + 0.25$	$\mu_0 - 0.25$	μ_0	$\mu_0 + 0.25$	$\mu_0 - 0.25$	μ_0	$\mu_0 + 0.25$		
(a) i. i. d. counts												
		EWMA			<i>1.156</i>	EWMA ^S $ x - 1 $			<i>0.349</i>	EWMA ^S $ x - 1 ^{1/4}$		<i>0.3146</i>
2	ZIP	506.6	462.0	149.7	139.4	257.2	481.5	54.2	81.0	124.9		
	NB	605.8	370.7	133.1	172.1	370.9	892.2	154.0	369.9	1001.2		
	oNB	171.9	135.1	75.6	45.2	67.2	103.8	52.2	86.9	163.2		
		EWMA			<i>1.805</i>	EWMA ^S $ x - 1 $			<i>0.1554</i>	EWMA ^S $ x - 1 ^{1/4}$		<i>0.0883</i>
5	ZIP	342.6	407.5	261.9	116.2	143.9	170.2	22.7	24.7	26.8		
	NB	444.7	370.8	205.3	267.3	369.8	522.7	260.0	370.1	537.2		
	oNB	130.2	124.7	94.8	42.9	51.3	59.1	55.5	68.7	87.3		
(b) AR(1) counts with $\rho = 0.5$												
		EWMA			<i>1.855</i>	EWMA ^S $ x - 1 $			<i>0.45</i>	EWMA ^S $ x - 1 ^{1/4}$		<i>0.4415</i>
2	ZIP	1287.7	505.7	238.0	108.3	167.0	266.3	90.6	139.7	219.4		
	NB	770.9	369.7	200.4	187.4	370.7	710.6	182.7	370.7	768.8		
	oNB	288.9	178.8	115.2	61.1	93.5	141.8	75.4	123.1	210.1		
		EWMA			<i>2.78</i>	EWMA ^S $ x - 1 $			<i>0.177</i>	EWMA ^S $ x - 1 ^{1/4}$		<i>0.1105</i>
5	ZIP	502.7	408.0	284.2	147.8	178.4	214.4	93.6	110.2	131.1		
	NB	510.8	369.6	242.5	278.0	370.8	494.2	276.7	370.2	492.8		
	oNB	183.8	156.4	124.4	60.1	71.6	83.0	78.5	97.1	122.0		

Notes: In-control ARL printed in bold font, CL L shown in italic font.
“EWMA” = ordinary EWMA; “EWMA^S” = Stein EWMA,
where weight functions $f(x) = |x - 1|$ and $|x - 1|^{1/4}$.

Interpre- tation:	sole mean change	pure distrib. change	zero inflation
			overdispersion

rather different ARL performance, they can be used for a kind of targeted diagnosis, i. e., one can conclude from the observed pattern of alarms on the type of out-of-control situation. For example, if the chart with $f(x) = |x - 1|^{1/4}$ signals first, we conclude on zero inflation.

Next, let us look at parts (b) of Tables 1–2, i. e., on the case of positively correlated counts. Note that in Table 2, the overdispersed NB-counts are still generated by the NB-IINAR(1) model (3), whereas the ZIP-INAR(1) model was used for zero inflation, i. e., model (2) with ZIP-innovations (ϵ_t). In most cases in parts (b), CLs have to be increased and the charts’ ARL performances get worse. But it still holds that the Stein EWMA charts are superior under overdispersion or zero inflation. As the only difference, the ARL performances of both Stein EWMA charts are now quite similar under

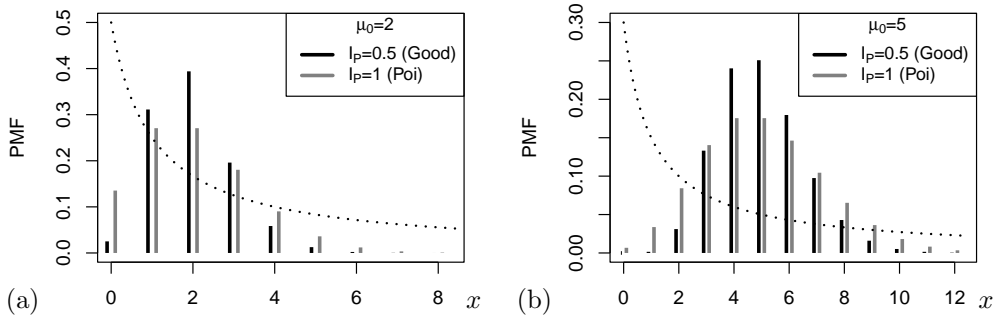


Figure 1: PMF plots for Good with $I_P = 0.5$ vs. Poi, for (a) $\mu_0 = 2$ and (b) $\mu_0 = 5$. Dotted line proportional to $1/(x + 1)$.

zero inflation in the Bin-case, but not for the NB-case. So altogether, the conclusions done for i. i. d. counts still apply, but with generally increased out-of-control ARLs due to the serial dependence.

4.2 Underdispersion

Underdispersion is the opposite phenomenon to overdispersion, i. e., the PMF is concentrated more closely around the mean. While there are hardly any models for underdispersion of bounded counts, the underdispersion of unbounded counts received more interest in the literature. For the subsequent simulations, we use the Good distribution (see Weiß, 2018, Appendix A) for generating underdispersion relative to the Poi-distribution (see Table 3), whereas for underdispersion relative to an NB-distribution, we use either an NB-distribution with less dispersion or the Poi-distribution (see Table 4). It quickly gets clear from Tables 3–4 that underdispersion is quite demanding for process monitoring. If looking first at the ordinary EWMA chart (first columns of blocks), we recognize severely increasing ARLs in the presence of underdispersion. This is reasonable as fluctuations of the DGP are reduced such that small mean shifts (we have ± 0.25) hardly lead to a violation of the CLs. The second columns in Tables 3–4 refer to the Stein EWMA charts (9) and (10), where we used $f(x) = 1/(x + 1)$ as recommended by Weiß et al. (2023) in the context of GoF-tests. While this chart indeed performs well for the low mean $\mu = 2$, the ARL performance is very bad for $\mu = 5$, again demonstrating that process monitoring in the presence of underdispersion is quite demanding. To better understand these difficulties and to find a solution, let us look at Figure 1, where we visualize the effect of underdispersion (black) compared to the in-control model (grey) by PMF plots. It can be seen that the strongest deviations are in a small area below μ_0 .

Table 3: Simulated ARLs of ordinary EWMA and Stein EWMA chart for Poi-counts. Good with $I_P = 3/4$ (first row) and $I_P = 1/2$ (second row).

μ_0	$\mu =$	$\mu_0 - 0.25$	μ_0	$\mu_0 + 0.25$	$\mu_0 - 0.25$	μ_0	$\mu_0 + 0.25$	$\mu_0 - 0.25$	μ_0	$\mu_0 + 0.25$		
(a) i. i. d. counts												
		EWMA		<i>0.877</i>	EWMA ^S		$1/(x+1)$	<i>0.223</i>	EWMA ^S		$p_P(x+2)$	<i>0.608</i>
2	Poi	252.6	369.1	106.1	274.6	368.9	470.8	538.9	370.3	271.7		
	Good	622.4	948.9	158.5	96.9	142.3	249.5	90.7	71.4	60.5		
	Good	3611.8	6346.9	380.6	32.3	42.2	63.0	29.1	26.2	24.3		
		EWMA		<i>1.388</i>	EWMA ^S		$1/(x+1)$	<i>0.1775</i>	EWMA ^S		$p_P(x+2)$	<i>0.293</i>
5	Poi	309.9	371.4	185.1	352.9	370.5	398.1	526.1	368.7	268.9		
	Good	1006.0	1015.9	327.2	$> 10^4$	$> 10^4$	$> 10^4$	228.4	149.3	106.4		
	Good	8154.5	7882.4	1168.9	$> 10^4$	$> 10^4$	$> 10^4$	52.5	40.1	33.2		
(b) AR(1) counts with $\rho = 0.5$												
		EWMA		<i>1.351</i>	EWMA ^S		$1/(x+1)$	<i>0.2467</i>	EWMA ^S		$p_P(x+2)$	<i>0.7235</i>
2	Poi	627.2	371.0	162.0	274.8	370.0	478.4	530.0	370.5	273.2		
	Good	2177.5	814.6	261.3	153.7	242.0	439.2	143.5	108.9	89.6		
	Good	$> 10^4$	2866.0	581.6	47.6	62.4	92.3	43.7	36.7	33.2		
		EWMA		<i>2.123</i>	EWMA ^S		$1/(x+1)$	<i>0.1707</i>	EWMA ^S		$p_P(x+2)$	<i>0.345</i>
5	Poi	432.2	369.8	236.3	332.3	370.1	395.3	514.5	370.1	280.7		
	Good	1369.3	909.2	446.1	2652.2	4029.5	5159.4	226.6	161.8	122.0		
	Good	$> 10^4$	4264.3	1402.0	1856.0	6087.1	$> 10^4$	69.8	53.9	44.3		

Notes: In-control ARL printed in bold font, CL L shown in italic font.
 “EWMA” = ordinary EWMA; “EWMA^S” = Stein EWMA,
 where weight functions $f(x) = 1/(x+1)$ and $p_P(x+2)$.

Interpre- tation:	sole mean change	pure distrib. change	increasing underdispersion

For $\mu_0 = 2$ in (a), the main deviations happen for $x \in \{0, 1, 2\}$. In fact, $f(x) = 1/(x+1)$ (symbolized by the dotted graphs in Figure 1) indeed puts most weight to this region, which explains the good ARL performance in this case. For $\mu_0 = 5$ in (b), however, the main deviations are for $x \in \{2, \dots, 5\}$. As $f(x) = 1/(x+1)$ puts relatively low weight into this region, we now get a poor ARL performance.

To get a good performance regarding underdispersion, Figure 1 suggests to put most weight somewhat below the in-control mean, which leads to the following idea. The in-control PMF itself (plotted in grey in Figure 1), interpreted as a weight function, puts most weight around the mean of the in-control distribution. Thus, we may just shift this PMF downwards to move most weight below the mean. Inspired by Figure 1 and some simulation experiments, the idea was developed to define $f(x)$ by simply shifting the in-control PMF by 2. More precisely, for the in-control Poi-model of Ta-

Table 4: Simulated ARLs of ordinary EWMA and Stein EWMA chart for NB-counts with $I_P = 5/3$. Underdispersed NB (“uNB”) with $I_P = 4/3$.

μ_0	$\mu =$	$\mu_0 - 0.25$	μ_0	$\mu_0 + 0.25$	$\mu_0 - 0.25$	μ_0	$\mu_0 + 0.25$	$\mu_0 - 0.25$	μ_0	$\mu_0 + 0.25$				
(a) i. i. d. counts														
		EWMA			<i>1.156</i>	EWMA ^S			$1/(x+1)$	<i>0.2215</i>	EWMA ^S		$p_N(x+2)$	<i>0.4163</i>
2	NB	605.8	370.7	133.1		240.3	371.5	590.6		367.7	370.3	325.2		
	uNB	1531.2	799.1	202.7		280.0	380.5	568.9		315.1	213.5	152.7		
	Poi	5998.4	3237.7	429.8		106.1	128.8	179.9		93.7	70.8	57.3		
		EWMA			<i>1.805</i>	EWMA ^S			$1/(x+1)$	<i>0.165</i>	EWMA ^S		$p_N(x+2)$	<i>0.22</i>
5	NB	444.7	370.8	205.3		301.9	369.1	452.9		399.3	369.1	328.4		
	uNB	1072.6	840.9	372.4		1185.9	1531.8	1921.6		455.4	313.1	226.8		
	Poi	4236.6	3623.7	986.3		7006.1	$> 10^4$	$> 10^4$		132.6	96.9	76.5		
(b) AR(1) counts with $\rho = 0.5$														
		EWMA			<i>1.855</i>	EWMA ^S			$1/(x+1)$	<i>0.2412</i>	EWMA ^S		$p_N(x+2)$	<i>0.4626</i>
2	NB	770.9	369.7	200.4		266.3	369.8	514.0		440.5	369.8	293.9		
	uNB	1797.1	685.4	315.4		233.3	319.1	441.7		248.6	177.5	137.2		
	Poi	$> 10^4$	2329.1	713.9		103.7	136.9	190.5		87.6	68.6	58.2		
		EWMA			<i>2.78</i>	EWMA ^S			$1/(x+1)$	<i>0.1727</i>	EWMA ^S		$p_N(x+2)$	<i>0.247</i>
5	NB	510.8	369.6	242.5		308.7	370.7	442.5		414.8	370.0	306.6		
	uNB	1148.0	700.0	420.9		787.5	973.5	1222.5		329.4	241.2	191.5		
	Poi	4918.5	2317.8	1082.8		1689.4	2741.1	4019.6		124.0	96.6	78.9		

Notes: In-control ARL printed in bold font, CL L shown in italic font.
“EWMA” = ordinary EWMA; “EWMA^S” = Stein EWMA,
where weight functions $f(x) = 1/(x+1)$ and $p_N(x+2)$.

Interpre- tation:	sole mean change		pure distrib. change		increasing underdispersion

ble 3, we use $p_P(x+2)$ as the weight function, and $p_N(x+2)$ for the NB-model of Table 4. Here, $p_P(\cdot)$ and $p_N(\cdot)$ abbreviate the PMFs of the in-control Poi- and NB-distribution, respectively. The computed chart designs and ARLs are summarized in the respective third column of Tables 3–4. We now get notably decreasing ARLs for increasing underdispersion in any scenario, both under i. i. d. and AR(1)-like counts.

5 An Illustrative Data Application

Weiß & Testik (2015) analyzed a large set of daily count time series referring to registrations in the emergency department of a children’s hospital. More precisely, these emergency counts were determined per 5-min interval from 08:00:00 to 23:59:59 on a day (so length $T = 192$), and the full set of time series covers the period from February 13 to August 13, 2009. Weiß & Testik

(2015) used the sixteen time series from February 13 to 28 to develop the in-control model (Phase-I analysis), namely a Poi-INAR(1) model with in-control mean $\mu_0 = 2.1$ and dependence parameter $\rho_0 = 0.78$. Control charts based on this model were then applied to prospective process monitoring (Phase-II application). While most Phase-II series did not contradict the in-control model, Weiß & Testik (2015) recognized a few unusual days, two of which shall now serve as illustrative data examples.

Let us start our analyses by designing the control charts based on the in-control model. To make the results consistent with Section 4, the CLs of each chart are chosen such that the in-control ARL is close to 370. On the one hand, we consider the c-chart and the ordinary EWMA chart (1) as competitors. On the other hand, the new Stein EWMA chart (9) was used together with four weight function: $f(x) = |x - 1|$ and $|x - 1|^{1/4}$ for indicating possible overdispersion or zero inflation, and $f(x) = 1/(x + 1)$ and $p_P(x + 2)$ for underdispersion. While the ARLs of the c-chart are computed numerically exactly by using the Markov-chain approach (see Weiß, 2018, Section 8.2.2), we again used simulations with 10^4 replications for the remaining charts. Here, the c-chart is most difficult to design due to discreteness; the best design has LCL = 0 and UCL = 6 (so an only one-sided design, where counts $X_t > 6$ cause an alarm) and $ARL_0 \approx 326.2$. The EWMA chart designs (again with $\lambda = 0.1$) are truly two-sided, namely

- EWMA (1) with $L = 1.851$ and $ARL_0 \approx 370.3$;
- Stein EWMA (9) with $f(x) = |x - 1|$, $L = 0.848$, $ARL_0 \approx 370.5$;
- Stein EWMA (9) with $f(x) = |x - 1|^{1/4}$, $L = 0.829$, $ARL_0 \approx 370.5$;
- Stein EWMA (9) with $f(x) = 1/(x + 1)$, $L = 0.2994$, $ARL_0 \approx 370.5$;
- Stein EWMA (9) with $f(x) = p_P(x + 2)$, $L = 0.9594$, $ARL_0 \approx 370.2$.

As a first illustrative example, we apply these control charts to the emergency counts collected on March 28, 2009, see Figure 2. The c-chart triggers an alarm at $t = 23$, the ordinary EWMA only rather late at $t = 171$, both indicating that the in-control model is violated. The situation gets more clear if looking at the four Stein EWMA charts in Figure 2. The charts in (c) and (d) both trigger a very early alarm at $t = 6$, whereas those of (e) and (f) do not trigger an alarm at all. This indicates that we are confronted with overdispersion and zero inflation. In fact, comparing the sample properties of the emergency series from March 28, 2009, to the in-control model, we note a slight increase in the mean μ (from 2.1 to ≈ 2.323) and a substantial

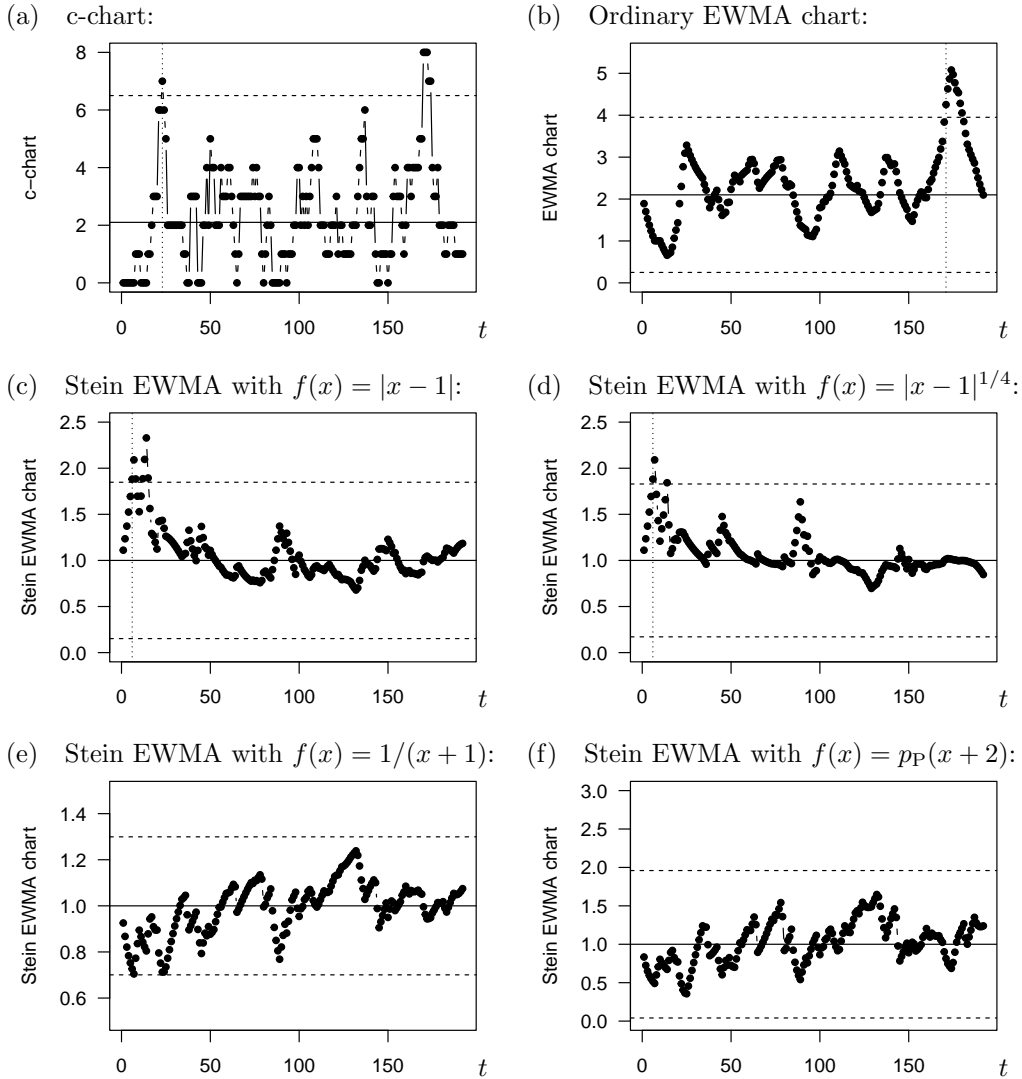


Figure 2: Emergency counts from March 28, 2009, see Section 5: c-chart in (a), ordinary EWMA chart in (b), and different Stein EWMA charts in (c)–(f). CLs as dashed lines, solid center line, and first alarm at dotted line.

increase in dispersion I_P (from 1 to ≈ 1.312). Furthermore, the number of zeros equals 27, being larger than 23.5 as expected under the in-control model. So the Stein EWMA charts gave a clear diagnosis of the type of out-of-control situation. In addition, their alarm at $t = 6$ was not only much faster than those of c-chart and ordinary EWMA chart, but also than those of the control charts in Weiß & Testik (2015) (these trigger at $t = 48$ and $t = 50$, respectively).

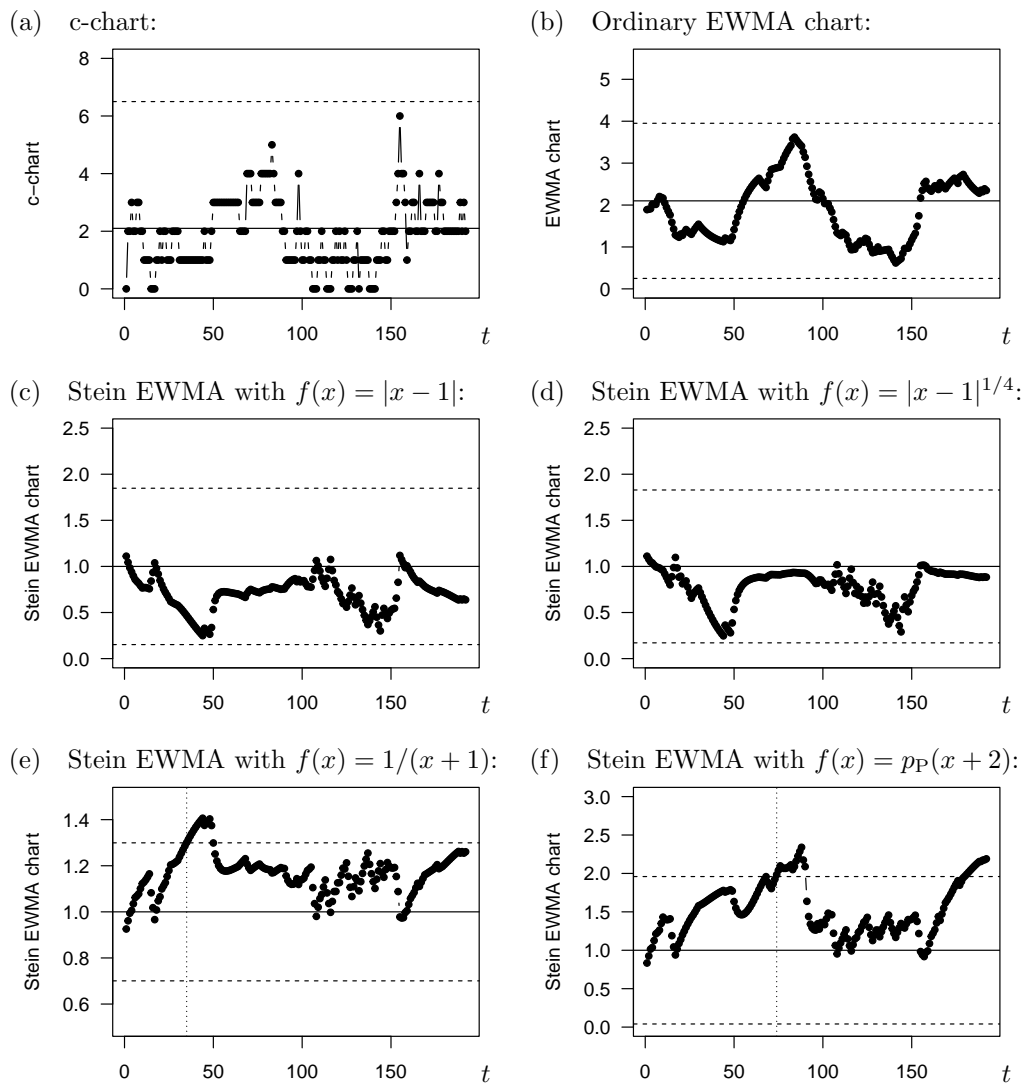


Figure 3: Emergency counts from July 16, 2009, see Section 5: c-chart in (a), ordinary EWMA chart in (b), and different Stein EWMA charts in (c)–(f). CLs as dashed lines, solid center line, and first alarm at dotted line.

As the second illustrative example, see Figure 3, we consider the emergency counts from July 16, 2009, where no results are reported by Weiß & Testik (2015). This time, neither c-chart nor ordinary EWMA chart trigger an alarm, so the user would conclude that the emergency series is in control. Looking at the Stein EWMA charts, however, the ones in (e) and (f) signal at times $t = 35$ and $t = 74$, respectively, so we seem to be confronted with underdispersion. In fact, the sample value of I_P is ≈ 0.710 being notably

smaller than 1, but also the mean has decreased from 2.1 to ≈ 1.911 . As we know from Section 4.2, the ordinary EWMA chart is hardly able to detect mean shifts in the presence of underdispersion, so the novel Stein EWMA charts constitute a welcome complement for this scenario.

6 Conclusions and Future Research

For the monitoring of either Poi-, NB-, or Bin-counts, corresponding Stein EWMA charts were proposed, which are constructed by utilizing the respective Stein identity. Their ARL performance was investigated by simulations, both for i. i. d. and AR(1)-like counts. It turned out that overdispersion is best detected by using the linear weights $f(x) = |x - 1|$, and zero inflation by the root weights $f(x) = |x - 1|^{1/4}$. Count monitoring in the presence of underdispersion, however, turned out to be quite demanding. While the ordinary EWMA charts performs very poorly in this case, the Stein EWMA chart with inverse weights $f(x) = 1/(x + 1)$ has appealing out-of-control ARLs for low counts. Even more promising is the weight function obtained by a downward shift of the in-control PMF. These findings were also confirmed by the data example on emergency counts. Nevertheless, it appears that the monitoring of underdispersion requires additional research activity.

There are further directions for future research. As cumulative sum (CUSUM) charts often show a better out-of-control performance than EWMA charts, it would be relevant to develop and investigate Stein CUSUM charts for count processes. Here, a residuals-based approach in analogy to Weiß & Testik (2015) would be attractive, as this would not only be applicable to Poi-, NB-, or Bin-marginals, but also to in-control models having a Poi-, NB-, or Bin-conditional distribution. Furthermore, Stein EWMA or CUSUM charts would also be interesting for continuously distributed variables data; for this case, Stein identities can be found in Sudheesh (2009); Landsman & Valdez (2016), among others.

Acknowledgments

The author thanks the two referees for their useful comments on an earlier draft of this article. This research was funded by the Deutsche Forschungsgemeinschaft (DFG, German Research Foundation) – Projektnummer 437270842.

References

- Aleksandrov, B., Weiß, C.H., Jentsch, C. (2022a) Goodness-of-fit tests for Poisson count time series based on the Stein–Chen identity. *Statistica Neerlandica* **76**(1), 35–64.
- Aleksandrov, B., Weiß, C.H., Jentsch, C., Faymonville, M. (2022b) Novel goodness-of-fit tests for binomial count time series. *Statistics* **56**(5), 957–990.
- Alevizakos, V., Koukouvinos, C. (2020) A comparative study on Poisson control charts. *Quality Technology & Quantitative Management* **17**(3), 354–382.
- Anastasopoulou, M., Rakitzis, A.C. (2022a) EWMA control charts for monitoring correlated counts with finite range. *Journal of Applied Statistics* **49**(3), 553–573.
- Anastasopoulou, M., Rakitzis, A.C. (2022b) Monitoring a BAR(1) process with EWMA and DEWMA control charts. In Tran (ed): *Control Charts and Machine Learning for Anomaly Detection in Manufacturing*, Springer Series in Reliability Engineering, Springer, Cham, 77–103.
- Betsch, S., Ebner, B., Nestmann, F. (2022) Characterizations of non-normalized discrete probability distributions and their application in statistics. *Electronic Journal of Statistics* **16**(1), 1303–1329.
- Borrór, C.M., Champ, C.W., Ridgón, S.E. (1998) Poisson EWMA control charts. *Journal of Quality Technology* **30**(4), 352–361.
- Chen, L.H.Y. (1975) Poisson approximation for dependent trials. *Annals of Probability* **3**(3), 534–545.
- Gan, F.F. (1990) Monitoring Poisson observations using modified exponentially weighted moving average control charts. *Communications in Statistics — Simulation and Computation* **19**(1), 103–124.
- Johnson, N.L., Kemp, A.W., Kotz, S. (2005) *Univariate Discrete Distributions*. 3rd edition, John Wiley & Sons, Inc., Hoboken, New Jersey.
- Knoth, S. (2006) The art of evaluating monitoring schemes — How to measure the performance of control charts? In Lenz & Wilrich (eds): *Frontiers in Statistical Quality Control 8*, Physica-Verlag, Heidelberg, 74–99.

- Knoth, S., Saleh, N.A., Mahmoud, M.A., Woodall, W.H., Tercero-Gómez, V.G. (2023) A critique of a variety of “memory-based” process monitoring methods. *Journal of Quality Technology* **55**(1), 18–42.
- Landsman, Z., Valdez, E.A. (2016) The tail Stein’s identity with applications to risk measures. *North American Actuarial Journal* **20**(4), 313–326.
- Montgomery, D.C. (2009) *Introduction to Statistical Quality Control*. 6th edition, John Wiley & Sons, Inc., New York.
- Morais, M.C., Knoth, S. (2020) Improving the ARL profile and the accuracy of its calculation for Poisson EWMA charts. *Quality and Reliability Engineering International* **36**(3), 876–889.
- Morais, M.C., Knoth, S., Weiß, C.H. (2018) An ARL-unbiased thinning-based EWMA chart to monitor counts. *Sequential Analysis* **37**(4), 487–510.
- Qiu, P. (2014) *Introduction to Statistical Process Control*. CRC Press, Taylor & Francis Group, Boca Raton.
- Rakitzis, A.C., Castagliola, P., Maravelakis, P.E. (2015) A new memory-type monitoring technique for count data. *Computers & Industrial Engineering* **85**, 235–247.
- Stein, C. (1972) A bound for the error in the normal approximation to the distribution of a sum of dependent random variables. *Proceedings of the Sixth Berkeley Symposium on Mathematical Statistics and Probability* **2**, 583–602.
- Stein, C. (1986) *Approximate computation of expectations*. IMS Lecture Notes, Volume 7, Hayward, California.
- Sudheesh, K.K. (2009) On Stein’s identity and its applications. *Statistics & Probability Letters* **79**(12), 1444–1449.
- Sudheesh, K.K., Tibiletti, L. (2012) Moment identity for discrete random variable and its applications. *Statistics* **46**(6), 767–775.
- Weiß, C.H. (2008) Thinning operations for modelling time series of counts — a survey. *AStA Advances in Statistical Analysis* **92**(3), 319–341.
- Weiß, C.H. (2011) Detecting mean increases in Poisson INAR(1) processes with EWMA control charts. *Journal of Applied Statistics* **38**(2), 383–398.

- Wei, C.H. (2015) SPC methods for time-dependent processes of counts— a literature review. *Cogent Mathematics* **2**(1), 1111116.
- Wei, C.H. (2018) *An Introduction to Discrete-Valued Time Series*. John Wiley & Sons, Inc., Chichester.
- Wei, C.H. (2023) Control charts for Poisson counts based on the Stein–Chen identity. Accepted for publication in *Advanced Statistical Methods in Statistical Process Monitoring, Finance, and Environmental Science*, Springer, 2023. arXiv preprint at arXiv:2305.19006.
- Wei, C.H., Puig, P., Aleksandrov, B. (2023) Optimal Stein-type goodness-of-fit tests for count data. *Biometrical Journal* **65**(2), 2200073.
- Wei, C.H., Testik, M.C. (2015) Residuals-based CUSUM charts for Poisson INAR(1) processes. *Journal of Quality Technology* **47**(1), 30–42.